frontiers | Frontiers in Energy Research

ORIGINAL RESEARCH
published: 08 June 2022
doi: 10.3389/fenrg.2022.926342

Study of the Effect of the Driving Force on the Kinetics of CO_2 Hydrate Growth in Coal Particles

Liu Chuanhai[1,2]*, *Chen Ran*[1,2], *Zhang Baoyong*[1,2], *Wu Qiang*[1,2], *Zhang Qiang*[1,2] and *WU Qiong*[1,2]

[1]Department of Safety Engineering, Heilongjiang University of Science and Technology, Harbin, China, [2]National Central Laboratory of Hydrocarbon Gas Transportation Pipeline Safety, Harbin, China

OPEN ACCESS

Edited by:
Liu Zhen,
Shandong University of Science and Technology, China

Reviewed by:
Xiao Li,
China University of Mining and Technology, China
Leilei Si,
Henan Polytechnic University, China
Zhenyang Wang,
Shandong University of Science and Technology, China

***Correspondence:**
Liu Chuanhai
liuchuanhai0429@126.com

Specialty section:
This article was submitted to Carbon Capture, Utilization and Storage, a section of the journal Frontiers in Energy Research

Received: 22 April 2022
Accepted: 23 May 2022
Published: 08 June 2022

Citation:
Chuanhai L, Ran C, Baoyong Z, Qiang W, Qiang Z and Qiong WU (2022) Study of the Effect of the Driving Force on the Kinetics of CO_2 Hydrate Growth in Coal Particles. Front. Energy Res. 10:926342. doi: 10.3389/fenrg.2022.926342

Coal and gas outbursts are geological disasters occurring in the process of coal mining that can cause serious casualties and economic losses, among which CH_4 is the main component of coal mine gas. However, there are still many coal seams around the world that are dominated by CO_2. Although the frequency of CO_2 gas outburst accidents is relatively low, CO_2 outbursts are very violent, notably difficult to control and highly dangerous. The application of hydration curing technology to reduce the pressure and gradient of CO2 gas in the coal can effectively reduce the occurrence of coal and CO_2 outburst. Accordingly, in this paper, experimental studies on the growth kinetics of CO_2 hydrate with three driving forces (2, 2.5, 3 MPa) were carried out under four different coal particle sizes (C1: 0.425–0.850 mm, C2: 0.250–0.425 mm, C3: 0.180–0.250 mm, C4: 0–0.180 mm) to obtain kinetic parameters such as gas consumption, growth rate, and heat of decomposition during the synthesis of CO_2 hydrate. The results show that the hydrate nucleation time in the same particle size system does not follow the same decreasing trend with increasing driving force. Gas consumption of CO_2 hydrates in the same particle size system increased with increasing driving force, and there exists a critical value regarding the effect of the driving force on CO_2 hydrate generation in coal particles with the particle size. Under the same temperature conditions, increasing the driving force in the particle size system could increase the CO_2 hydrate growth rate. With decreasing coal particle size and increasing driving force, the promoting effect gradually exceed the inhibiting effect, which promote CO_2 hydrate formation. Through linear fitting, an equation of the average growth rate of CO_2 hydrates versus the driving force for the C1-C4 systems is fitted to provide a reference to predict the average CO_2 hydrate growth rate. In the same medium, with increasing driving force, more heat is required for complete decomposition, which remains relatively stable, and the heat of decomposition of CO_2 hydrates is the highest in the C1 medium, indicating that the presence of CO_2 hydrates in the C1 system represents the most stable state.

Keywords: CO_2 hydrates, gas consumption, growth rate, heat of decomposition, coal and gas outburst

INTRODUCTION

Coal energy is widely used in heating, power generation and other industries, accounting for 56% of the total primary energy consumption in China in 2021 (Hu, 2022). As the demand for coal energy increases year by year, the intensity and depth of coal mining have gradually increased, causing frequent geological disasters such as coal and gas outbursts. Coal and gas outbursts are dynamic phenomena in which coal and gas violently erupt from coal seams within a short period in the underground mining process, which can cause serious economic losses and casualties (Xu and Jiang, 2017; Si et al., 2021a). Therefore, regarding the prevention and control of coal and gas outburst disasters, Wu Qiang et al. (Wu et al., 2005) proposed mine gas hydration curing technology (the principle is shown in **Figure 1**). By injecting high-pressure and low-temperature water into a coal seam, CH_4 and CO_2 are hydrated and cured under high-pressure and low-temperature conditions to produce mine gas hydrates, thus reducing the mine gas content and pressure in the coal seam, and in the process of coal mining, because decomposition of solid mine gas hydrates absorbs much heat, the heat transfer coefficient of the surrounding rock of the coal seam is low, which cannot meet the heat requirements for mine gas hydrate ablation within a short time. Therefore, it is difficult to rapidly melt and decompose mine gas hydrates when breaking coal and forming high-pressure mine gas flows to prevent and control coal and gas outbursts.

CH_4 is the main component of coal mine gas in outburst-prone coal seams, but there remain many coal seams worldwide dominated by CO_2. Although coal and CO_2 outbursts occur relatively infrequently, researchers have pointed out that CO_2 outbursts are very violent, notably difficult to control and highly dangerous (Wu et al., 2010; Yang et al., 2016; Black, 2019). For example, the largest coal and gas outburst disaster ever recorded in Australia involved a CO_2 outburst in the Collinsville State Mine, which ejected 500 tons of coal and released approximately 14,000 m^3 of CO_2. The Metropolitan colliery in Australia also experienced a CO_2 outburst in 2017, ejecting 200 tons of coal and releasing approximately 11,500 m^3 of CO_2 (Black, 2019). The coal fields in China where CO_2 outbursts have occurred include the Yaojie coal field in Gansu, the Yingcheng coal field in Jilin, and the Helong coal field (Hou and Lu, 2000; Wang et al., 2009; Li et al., 2011). Among these coal fields, the CO_2 outburst volume in the Yaojie coal field reached as high as 240,000 m^3, and the outburst ejected 1,030 tons of coal and rock only on the day of the accident (Tao et al., 1992).

The application of hydration curing technology can theoretically effectively control the occurrence of CO_2 outburst accidents, but because the growth process of CO_2 hydrates entails continuous mass and heat transfer, there are usually limitations including a long induction time, low generation rate, and high phase equilibrium thermodynamic conditions in CO_2 hydrate generation (Sun et al., 2015; Li et al., 2019; Dai et al., 2020; Fan et al., 2020; Cao et al., 2021). Therefore, Chinese and foreign researchers have performed many experiments regarding the formation of CO_2 hydrates in noncoal systems. Liu Ni et al. (Liu et al., 2015) conducted a study of the kinetics of CO_2 hydrate generation in an Al_2O_3 nanoparticle system and found that there exists a certain optimal particle size value leading to the shortest CO_2 hydrate generation induction time and the largest amount of gas storage. Montazeri et al. (Montazeri et al., 2019) also found that there occurs an optimal value regarding the effect of the nanoparticle concentration on the hydrate generation rate and induction time by studying the process of CO_2 hydrate generation in boehmite nanoparticle systems, thus maximizing energy savings. Bai et al. (Bai et al., 2020) studied the formation pattern and distribution characteristics of CO_2 hydrates, and the results indicated that under nonliquefaction conditions, a hydrate film first emerged on the reactor wall, but as the initial temperature was reduced and liquefaction conditions were

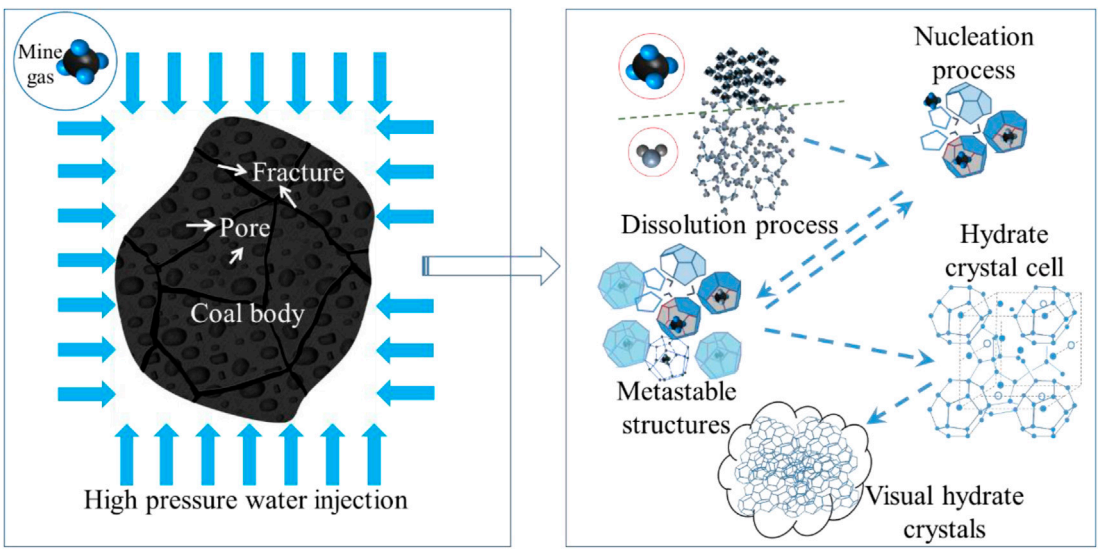

FIGURE 1 | Mine gas hydration curing reaction mechanism.

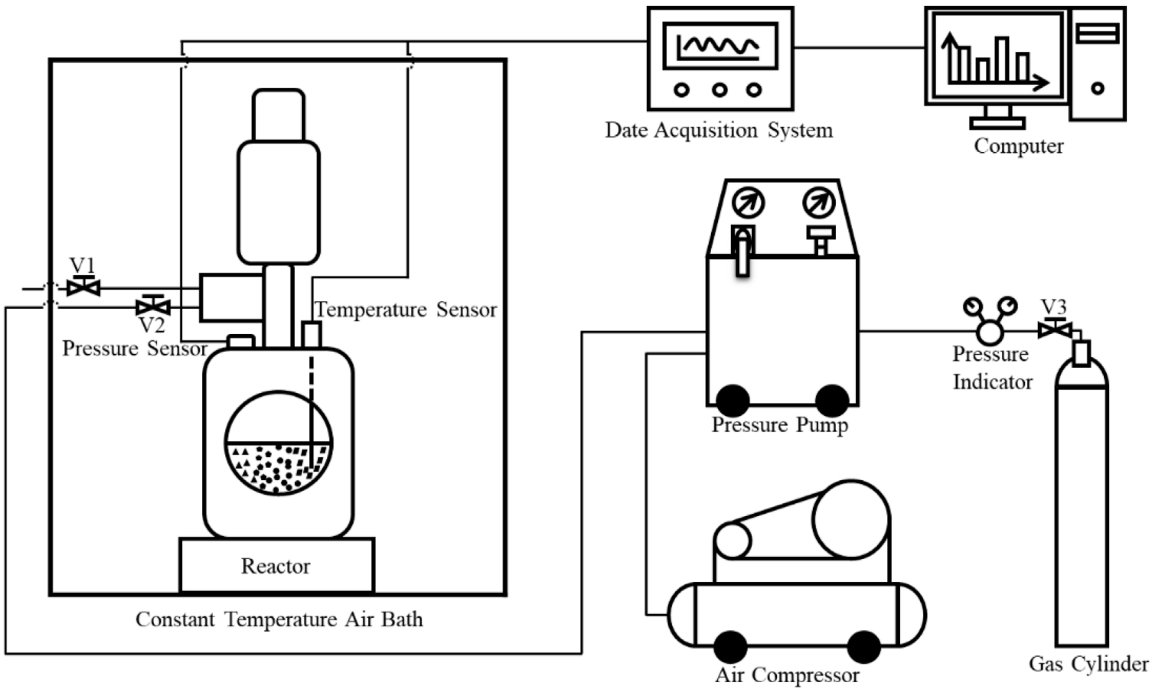

FIGURE 2 | Experimental apparatus for CO_2 hydrate growth kinetics in coal particles.

reached, hydrates were preferentially formed at the intersection of liquid CO_2 and water. Zhang et al. (Zhang et al., 2015) employed quartz sand and ice powder mixtures of different particle sizes to simulate the occurrence conditions of hydrates in the permafrost zone and concluded that the smaller the particle size of porous media within a certain particle size range, the higher the average hydrate formation rate and gas storage capacity of CO_2 hydrates are in the hydrate formation process. Seo et al. (Seo et al., 2005) investigated the process of CO_2 hydrate generation in porous silica gel with the nuclear magnetic resonance technique and demonstrated that water dispersed in silica gel reacted with CO_2 gas very rapidly, thus indicating that the process of CO_2 hydrate generation does not require excess water. Kang et al. (Kang and Lee, 2010) studied the process of CO_2 hydrate generation in silica gel with a pore size of 100 nm at different temperatures and pressures and concluded that the rate of CO_2 gas hydrate generation increased rapidly with increasing driving force. Thus, it can be found that current studies on the mechanism of CO_2 hydrate generation in porous media are mostly focused on solving the problem of CO_2 greenhouse gas emission reduction, but there are few reports on kinetic data of the CO_2 hydrate generation process in coal systems, let alone related literature.

In summary, the results of many studies have pointed out that the driving force and porous medium can promote synthesis of CO_2 hydrate. The reaction environment for coal and gas outburst disaster prevention based on the gas hydration solidification method is in the outburst coal body, which has a more complex multi-scale pore structure compared with other porous media (Si et al., 2021b), for which it is particularly important to explore in depth the analysis of factors influencing gas hydrate generation in coal particles. However, at present, there are few reports on the kinetics of the CO_2 hydrate generation process in coal particles in China and abroad, and there is a lack of data on CO_2 hydrate growth kinetics in coal particles. Accordingly, this paper adopted pressure driving force (ΔP), defined as the pressure value increased on the basis of phase equilibrium pressure (P_{eq}) during hydrate formation, and carried out experimental studies on CO_2 hydrate growth kinetics with three driving forces (2, 2.5, 3 MPa) under four different coal particle size conditions (C1: 0.425–0.850 mm, C2: 0.250–0.425 mm, C3: 0.180–0.250 mm, C4: 0–0.180 mm), respectively, and the effects of driving forces on kinetic parameters such as gas consumption, growth rate, and heat of decomposition during CO_2 hydrate synthesis in coal particles were discussed, which can provide experimental reference and theoretical basis for the selection of pressure driving forces for the realization of hydration curing technology to prevent and control coal and CO_2 protrusion in field applications.

EXPERIMENTAL SECTION

Apparatus and Materials

Figure 2 shows the experimental system of CO_2 hydrate growth kinetics in coal particles applied in the experiment. The apparatus mainly consists of a visual high-pressure reaction system, a gas booster system (all oil-free and water-free silent air compressors, air dehydrators, pressure pumps, and high-pressure pipelines), a thermostatic control system and a data acquisition system (industrial control computer, data acquisition module and temperature/pressure sensor).

Among these components, the visual high-pressure reaction system is the core part of the experimental device, the reactor body material is 316L stainless steel, the reaction system is equipped with a 3 cm diameter glass window, the effective volume is 1 L, the applicable temperature ranges from -10~50°C, and the ultimate pressure is 30MPa, similar to the properties of coal particles at the gas hydrate synthesis site. The power of silent air compressor is 6Kw, the gas exhaust capacity is 1000 L/min. The filtering precision of air de-waterer is 0.1 μm, the rate of water/oil removal is 99%, the air treatment quality is 0.48–1.54 Nm^3/min. The pressure pump can drive the gas source up to 0.69 MPa under maximum power conditions, and the pressure ranges from atmospheric pressure to the maximum rated value. Constant-temperature air bath is provided by Shanghai Ruiwen Instrument and Equipment Factory (temperature range: −10~60°C; accuracy ± 0.1°C). The temperature is precisely controlled with an intelligent microcomputer equipped with multichannel circulation ventilation, and the air duct is equipped with a heater and chiller to fully ensure that the working temperature within the chamber remained uniform. The data acquisition module displays store temperature and pressure data and a curve of changes over time through graphical software in real time, which is convenient for monitoring parameter changes in the experiment. The pressure and temperature of the experimental process are measured with pressure and temperature sensors, respectively. The measurement ranges are 0~25 MPa and −30~50°C, respectively, and the accuracy is ± 0.01 MPa and ± 0.1°C, respectively.

Experimental Procedure

In this paper, 12 groups of CO_2 hydrate growth kinetics experiments were carried out considering four particle sizes of coal samples at 5°C with driving forces of 2, 2.5, and 3 MPa. The variation trend of parameters such as gas consumption and growth rate during CO_2 hydrate synthesis in coal particles was studied. Pure water was homemade deionized water, and the purity of CO_2 gas used in the experiment was 99.99%.

1) Pure water was used to clean the reactor 2–3 times followed by drying. Typical outburst coal powder particles of different particle sizes were added to equal amounts of pure water, stirred evenly and added to the reactor. The coal powder was sieved in advance into the following particle size fractions: C1: 0.425~0.850 mm; C2: 0.250~0.425 mm; C3: 0.180~0.250 mm; C4: 0~0.180 mm Equipment pipelines were connected, and it was determined whether the connections were proper. The data acquisition system was activated, and the system software was operated.
2) Foam was applied to the pipeline connections for gas tightness testing, nitrogen at approximately 1 MPa was injected into the reactor, and it was determined whether there was a change in pressure under continuous bubble formation. If the above phenomenon did not occur, airtightness was ensured.
3) The thermostatic control system was activated, the constant-temperature air bath was set to 20°C, and when the temperature of the reactor remained stable at this temperature, 0.1 MPa experimental gas was injected into the reactor and pipeline, after which these components were emptied. Residual gas was purged from the reactor, and this step was repeated 3 times. Then, the gas booster system was activated, and CO_2 gas was injected to ensure that the pressure in the reactor reached the set value.
4) After the experiment was initiated, when the temperature and pressure values in the reactor remained unchanged, the constant-temperature air bath was set to 5°C to start cooling, and synthesis was sustained at this temperature for 48h. When the pressure in the reactor remained stable for a long time, the temperature was raised and maintained at 26°C to eliminate the memory effect, after which the temperature was lowered for the next experiment.

RESULTS AND DISCUSSION

CO_2 Hydrate Synthesis Process in Coal Particles

Nucleation and growth of CO_2 hydrate in coal particles are two key steps in the hydrate formation process, and the growth process can be subdivided into a fast growth phase, slow growth phase and dynamic equilibrium phase. The fast growth phase is mainly characterized by a rapid decrease in system pressure, and the duration varies from system to system. At the completion of the rapid growth phase, the experiment enters the next growth phase, the duration of this phase is slightly longer than that of the rapid growth phase, and the change in pressure drop is smaller. The experimental temperature still exhibits small increasing fluctuations within a certain range. Finally, the experiment reached dynamic equilibrium and was sustained, and the temperature and pressure basically remained stable during this phase.

Figure 3 shows P–T–t curves of the CO_2 hydrate generation process in the C1-C4 system. The figure shows that the system pressure decreases with decreasing experimental temperature, and the temperature of the four experimental systems remains stable at about 5°C. However, in the process of temperature reduction, all 12 groups of experiments for the C1-C4 system show a trend of temperature increase or slowing down of temperature decrease after the gas dissolution nucleation process. This occurs because the hydrate synthesis process is an exothermic process, and the system temperature increases due to the release of heat and then continues to decrease under the action of the external constant-temperature air bath. The temperature in Expt. Ⅰ-4-2 in the C4 system increase to a certain extent after dropping to approximately 9°C, which is caused by the exothermic generation of hydrates, indicating that the heat of reaction release at this time was much higher than the heat remove during the refrigeration system cycle. In addition, it can still be observed in the figure that the higher the pressure driving force of the four systems, the earlier the rapid temperature increase and subsequent decrease occur and the shorter the time require to reach the experimental pressure. Ideally, with increasing driving force, the induction time decreases, but the effects of the particle size, interfacial tension

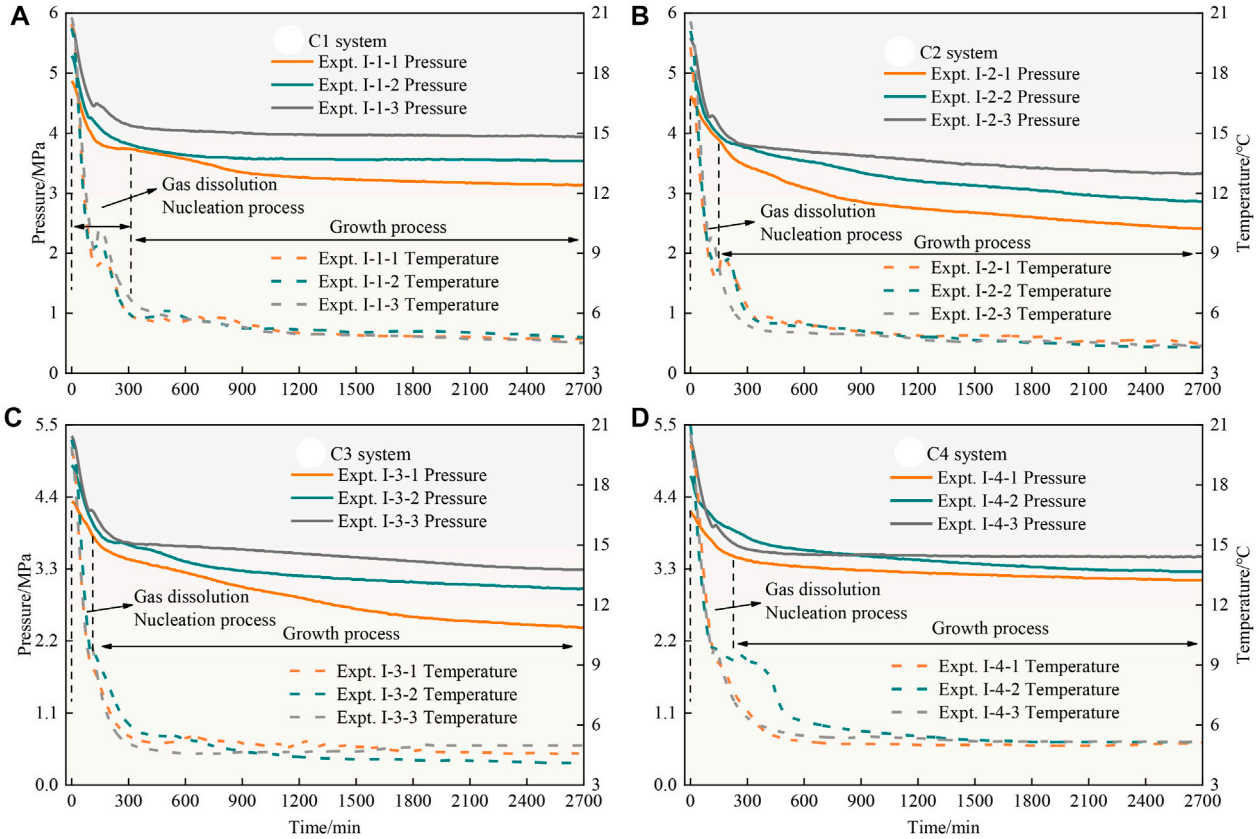

FIGURE 3 | P–T–t curves during CO_2 hydrate generation in the C1-C4 system.

and capillary coalescence cannot be excluded, so the induction time is not exactly the same for the different particle sizes.

Analysis of the Influence Law of CO_2 Hydrate Gas Consumption

Gas consumption is the central parameter reflecting the hydrate synthesis pattern. Hydrates are synthesized in a gas-consuming manner. Gas consumption is determined by the amount of gas change in the reactor for any given time t = 0~t. The number of moles of gas consumed is calculated with **Equation 1** (ZareNezhad et al., 2015; Zheng et al., 2019).

$$\Delta n_g = \left[\left(\frac{PV}{ZRT}\right)_{G,0} - \left(\frac{PV}{ZRT}\right)_{G,t}\right] \tag{1}$$

Where Δn_g is the gas consumption at moment t (mmol), P, V and T are the pressure (MPa), gas volume (cm^3) and temperature(K) in the reactor, respectively, R is the ideal gas constant (8.314 $J{\cdot}K^{-1}{\cdot}mol^{-1}$), and Z is the gas compression factor, which is calculated with gas compression factor calculation program version 1.0.

Since different initial water injections are used in the experiment, the gas consumption can be further divided by the number of moles of water(n_w) in the solution, yielding the normalized gas consumption, defined by **Eqn. 2** (Mech et al., 2016; Zheng et al., 2018).

$$\Delta N_t = \frac{\Delta n_g}{n_w} \tag{2}$$

Where ΔN_t is the normalized gas consumption at moment t (mmol/mol) and n_w is the number of moles of water (mol) in the solution.

Therefore, in this paper, the gas consumption of hydrates under the different pressure driving force conditions with time is calculated with **Eqns. 1**, **2**. The experimental results of the effect of the different pressure driving forces on the gas consumption of CO_2 hydrates in coal particles are listed in **Table 1**.

Figures 4A–D show the gas consumption of CO_2 hydrates in the C1-C4 systems under the different driving force conditions. The figure shows that the slopes of the gas consumption curves under the different pressure driving force conditions are different, and all of these curves show that the gas consumption rate of CO_2 hydrates rapidly rises when CO_2 hydrates are generated, and the gas consumption rate is relatively high at this stage. However, as the reaction proceeds, the gas consumption rate of CO_2 hydrates gradually decreases. The analysis suggests that because the density of CO_2 hydrates is lower than that of water, when CO_2 hydrates are further generated, hydrates can cover the

TABLE 1 | Consumption of gas of CO_2 hydrates in coal particles under the different driving forces.

Experimental system	Feed Gas	Medium	Particle size d/Mm	Experimental conditions		Driving force ΔP/MPa	Gas consumption *Nt*/(mmol/mol)
				Phase equilibrium pressure P_{eq}/MPa	Phase equilibrium temperature T/°C		
I-1-1	CO_2	C1	0.425~0.850	2.79	5	2	59.3
I-1-2						2.5	62.6
I-1-3						3	68.3
I-2-1		C2	0.250~0.425	2.59	5	2	59
I-2-2						2.5	61.1
I-2-3						3	63.7
I-3-1		C3	0.180~0.250	2.34	5	2	48.5
I-3-2						2.5	49.2
I-3-3						3	56.5
I-4-1		C4	0~0.180	2.24	5	2	31.1
I-4-2						2.5	47.5
I-4-3						3	62.8

Note: The medium comprises coal particles of C1: 0.425~0.850; C2: 0.250~0.425; C3: 0.180~0.250; C4: 0~0.180. The initial pressure in the kinetic experiment is $P = P_{eq} + \Delta P$.

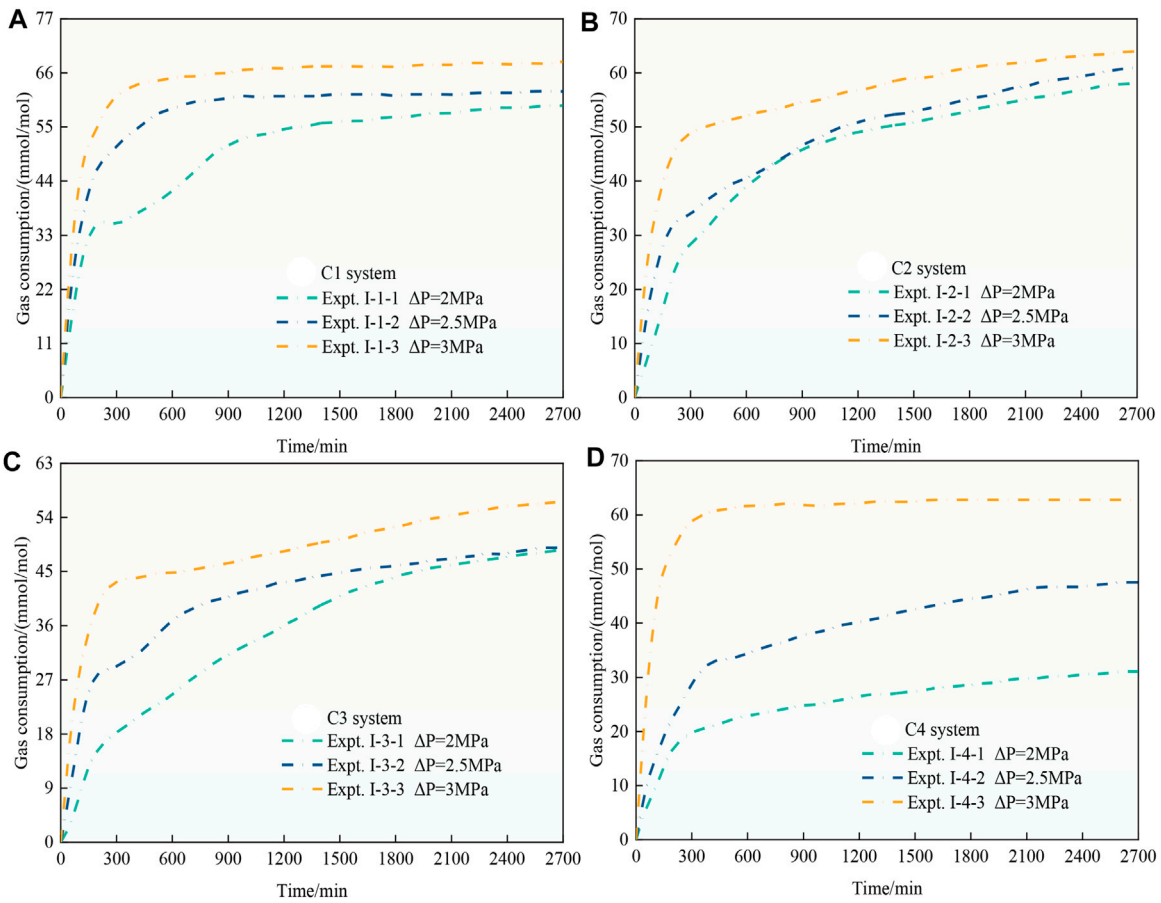

FIGURE 4 | Gas consumption of CO_2 hydrates in the C1-C4 systems.

surface of coal particles, and it is difficult for gas to diffuse into the interior of the coal particles, so the gas consumption rate of CO_2 hydrates gradually decreases and gas consumption gradually remains stable (CO_2 hydrates are basically no longer generated). Regarding CO_2 hydrates in the four particle size systems, the higher the driving force of the synthesis process is, the higher the slope of the gas consumption curve and the earlier the end of the CO_2 hydrate generation phase, indicating a

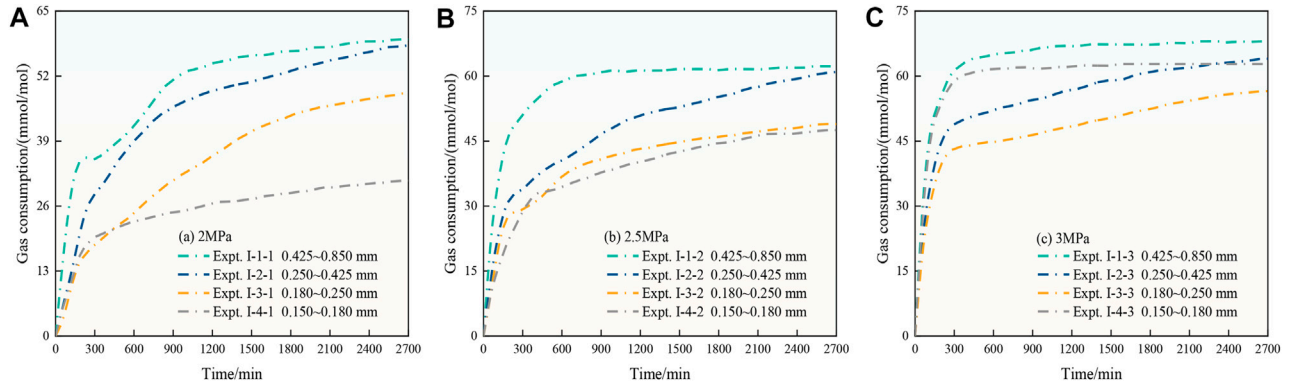

FIGURE 5 | Gas consumption of CO_2 hydrates in the 2, 2.5 and 3 MPa systems.

higher gas consumption rate. In the same particle size system, the gas consumption of CO_2 hydrates under all three pressure driving force conditions is ranked as $\Delta N_{t,3MPa}>\Delta N_{t,2.5MPa}>\Delta N_{t,2MPa}$, i.e., the gas consumption of CO_2 hydrates under the same particle size conditions increases with increasing driving force. This occurs because the driving force affects the gas diffusion process and increases the gas–liquid contact area in the later generation process, thus affecting gas consumption and CO_2 hydrate generation. However, the effect of the driving force on CO_2 hydrate generation varies among the different particle size systems, where the gas consumption under the 3 MPa (Expt. I-1-3) driving force in the C1 system is 1.09 and 1.15 times higher than that under the 2.5 MPa (Expt. I-1-2) driving force and 2 MPa (Expt. I-1-1) driving force, respectively. The gas consumption under the 3 MPa (Expt. I-2-3) driving force in the C2 system is 1.04 and 1.08 times higher than that under the 2.5 MPa (Expt. I-2-2) driving force and 2 MPa (Expt. I-2-1) driving force, respectively. The gas consumption under the 3 MPa (Expt. I-3-3) driving force in the C3 system is 1.15 and 1.16 times higher than that under the 2.5 MPa (Expt. I-3-2) driving force and 2 MPa (Expt. I-3-1) driving force, respectively. The gas consumption under the 3 MPa (Expt. I-4-3) driving force in the C4 system is 1.32 and 2.02 times higher than that under the 2.5 MPa (Expt. I-4-2) driving force and 2 MPa (Expt. I-4-1) driving force, respectively. With decreasing particle size, the effect of the driving force on gas consumption first decreases and then gradually increases. This phenomenon indicates that there exists a critical value regarding the effect of the driving force on CO_2 hydrate generation in coal particles with the change in particle size, above which the effect of the driving force on CO_2 hydrate generation gradually decreases with decreasing particle size, and below which the effect of the driving force on CO_2 hydrate generation gradually increases with decreasing in particle size.

Figures 5A–C show the CO_2 hydrate gas consumption in the 2, 2.5, and 3 MPa systems under the different particle sizes. As shown in **Figure 5A** and **Figure 5B**, the gas consumption of CO_2 hydrates gradually decreases with decreasing coal particle size. The reason for this phenomenon is that the diffusion and migration process of CO_2 gas inside the coal particle is hindered by the decrease in coal particle size, which leads to the inability of CO_2 to react with water deep within the coal particles to form hydrates, and thus, gas consumption decreases. However, as shown in **Figure 5C**, the gas consumption sequence of CO_2 hydrates of $\Delta N_{t,Expt.I\text{-}4\text{-}3}>\Delta N_{t,Expt.\ I\text{-}3\text{-}3}$ emerges, i.e., the gas consumption in the C4 particle size system is higher than that in the C3 particle size system under a 3 MPa driving force, which is the opposite to the phenomena in **Figure 5A** and **Figure 5B**. The analysis suggests that the reduction in particle size leads to an increase in the specific surface area of the coal particles, which greatly increases the gas–liquid contact area required for CO_2 hydrate growth, and the interfacial effect is especially prominent, which is favorable for CO_2 hydrate generation. Moreover, the promotion effect is further strengthened with increasing driving force, resulting in an increase in CO_2 hydrate gas consumption.

Analysis of the Influence Law of CO_2 Hydrate Average Growth Rate

The average growth rate is an important parameter of the overall synthesis process conditions of CO_2 hydrates, which can suitably reflect the kinetic behavior of CO_2 hydrate growth and can be calculated with **Equation3** (Mech et al., 2016; Zheng et al., 2018).

$$N_{r(t_{total})} = \frac{\Delta n_g}{t_{total}}. \tag{3}$$

Where $N_{r(t_{total})}$ is the ratio between the final amount of CO_2 hydrate production and the corresponding production time t_{total}.

The normalized average growth rate at each stage of the CO_2 hydrate synthesis process is calculated with the forward difference method given by **Equation4** (Zhong et al., 2016), where $N_{r(t)}$ is the normalized hydrate growth rate (mmol/mol/min) and Δt is the time interval (min).

$$N_{r(t)} = \frac{\left(\Delta n_g\right)_{t+\Delta t} - \left(\Delta n_g\right)_t}{\Delta t \cdot n_w} \tag{4}$$

Considering that CO_2 hydrate generation is not the same in the different particle size systems, the effect of the pressure driving force on CO_2 hydrate growth kinetics was accurately analyzed to avoid CO_2 hydrate generation from affecting the

TABLE 2 | Average growth rate of CO_2 hydrates in coal particles under the different driving forces.

Experimental system	Feed Gas	Medium	Particle size d/Mm	Driving force ΔP/MPa	Average growth rate over 300 min/(mmol/mol/min)	Average growth rate of the whole process/(mmol/mol/min)
I-1-1	CO_2	C1	0.425~0.850	2	0.11633	0.02196
I-1-2				2.5	0.17004	0.02319
I-1-3				3	0.20485	0.0253
I-2-1		C2	0.250~0.425	2	0.095	0.02185
I-2-2				2.5	0.11234	0.02263
I-2-3				3	0.16344	0.02359
I-3-1		C3	0.180~0.250	2	0.06113	0.01796
I-3-2				2.5	0.09683	0.01822
I-3-3				3	0.14479	0.02093
I-4-1		C4	0~0.180	2	0.06629	0.01152
I-4-2				2.5	0.09641	0.01759
I-4-3				3	0.19697	0.02326

Note: The medium comprises coal particles of C1: 0.425~0.850; C2: 0.250~0.425; C3: 0.180~0.250; C4: 0~0.180.

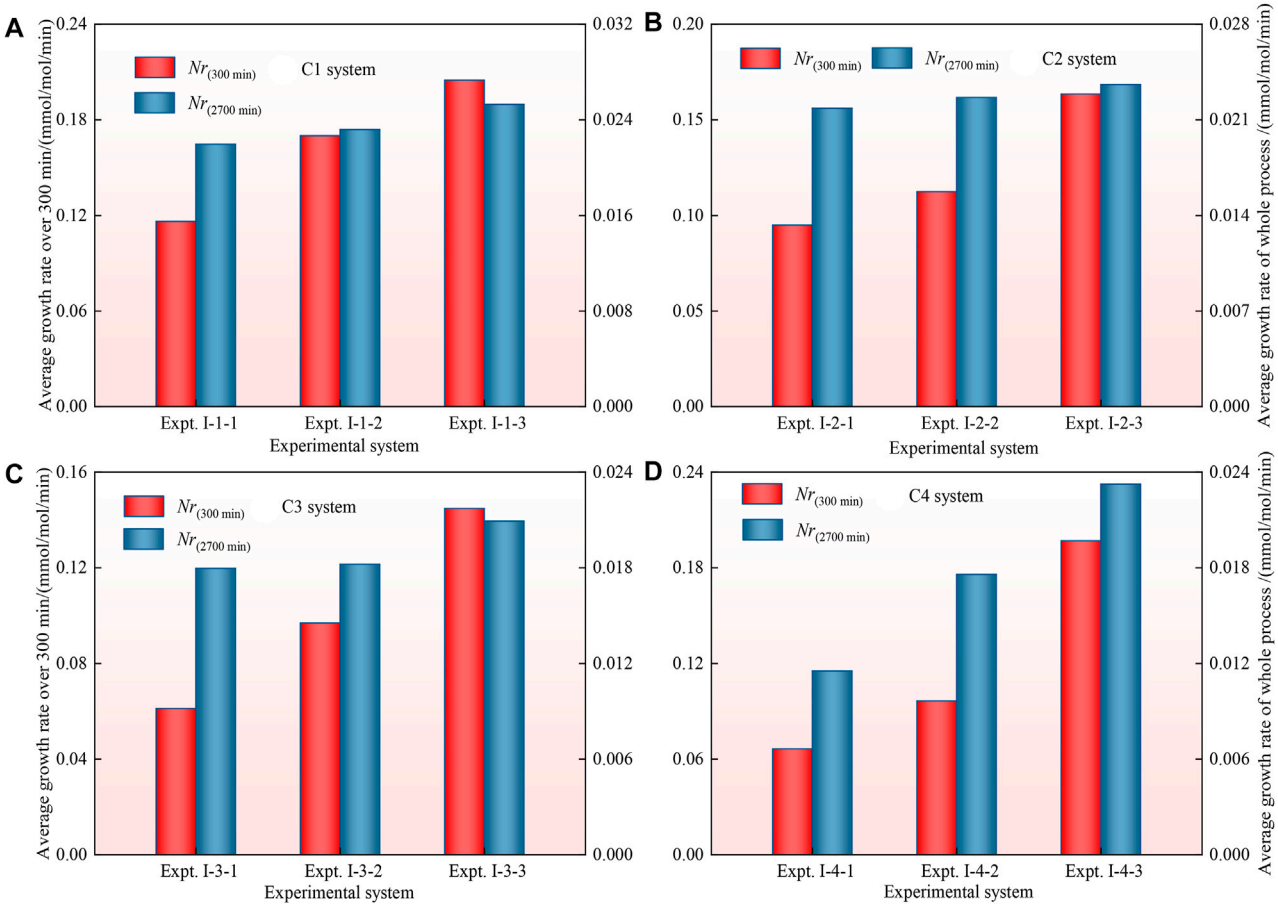

FIGURE 6 | Histogram comparing the average growth rate of CO_2 hydrates in the C1-C4 systems.

results of the experiments. The average growth rate of CO_2 hydrates in each system under the different driving forces was calculated in the experiment. The average growth rate during the first 300 min and the average growth rate of the whole process were considered to analyze the influence of the different driving forces on the formation process of CO_2 hydrates. The experimental results are provided in **Table 2**.

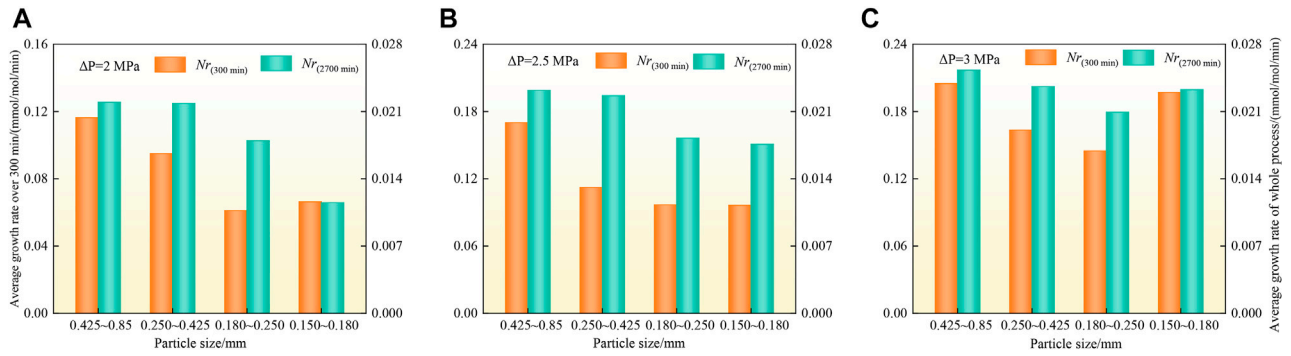

FIGURE 7 | Histogram comparing the average growth rate of CO_2 hydrates in the 2, 2.5 and 3 MPa systems.

The average growth rate of CO_2 hydrates in the C1-C4 systems is shown in **Figures 6A–B**. The average growth rate of CO_2 hydrates in the C1-C4 systems increases with increasing driving force. The average growth rate of CO_2 hydrates in the four particle size systems was ranked as $N_{r(\Delta P=3MPa)} > N_{r(\Delta P=2.5MPa)} > N_{r(\Delta P=2MPa)}$ over the first 300 min and the whole experiment under the three driving conditions, which indicated that the average growth rate of CO_2 hydrates increased with increasing driving force. The average growth rate was higher during the first 300 min of the experiment than that throughout the whole experiment, indicating that CO_2 hydrates were rapidly synthesized in large quantities during the first 300 min of the experiment. The analysis suggests that in a reaction system with a constant temperature and volume, the main water molecules and guest CO_2 molecules are adsorbed to form CO_2 hydrates at the gas–liquid interface in the upper layer of the coal particles first, and the Gibbs free energy of the system reaches a maximum value when CO_2 hydrate nuclei are formed. The higher the driving force of CO_2 hydrate generation, the more CO_2 hydrates are continuously synthesized rapidly along the direction of decreasing the molar Gibbs free energy, thus prompting the hydration reaction to rapidly proceed toward the lower layer of coal particles, and the CO_2 hydrates in the coal particles continuously increase, while the growth rate increases. However, as the reaction proceeds, when the particle size surface, pores between the coal particles and contact surface between the coal particles and CO_2 are occupied by CO_2 hydrates, the passage of CO_2 into the coal particles can become partially blocked, which increases the gas transport resistance and reduces the diffusion rate of gas. As the gas supply is insufficient, the CO_2 hydrate growth rate starts to decrease, resulting in a lower average growth rate throughout the experiment than that during the first 300 min of the experiment.

Figures 7A–C show that the average growth rate of CO_2 hydrates under the three driving force conditions decreases overall with decreasing particle size during the whole synthesis process. The analysis suggests that the average growth rate of CO_2 hydrates decreases with decreasing particle size of the coal particles, which hinders and inhibits the diffusion and migration of CO_2 in the pores of the coal particles to different degrees. However, with increasing driving force and decreasing coal particle size, the variation in the average growth rate of CO_2 hydrates gradually decreases or the growth rate of the CO_2 hydrate system even increases. The analysis suggests that during the process of CO_2 hydrate generation in the coal particle system, a decrease in particle size leads to obstruction of CO_2 gas diffusion and migration in the coal particles, which hinders CO_2 hydrate generation, but with increasing specific surface area and driving force of the coal particles, the promotion effect is strengthened and eventually exceeds the obstruction effect, which promotes CO_2 hydrate generation, resulting in the phenomenon of an increasing hydrate growth rate.

To predict the average growth rate of CO_2 hydrates under any driving force condition between 2 and 3 MPa in the C1-C4 particle size systems, the average growth rate of CO_2 hydrates in the C1-C4 systems is fitted with the driving force using linear fitting, and the fitting results are shown in **Figures 8A–D** and **Table3**. Among them, except for the general correlation of the whole process for the C3 system (correlation coefficient $R_{Nr(2700\ min)} = 0.63$), the rest of the fitting results show extremely strong or strong correlation. The construction of these fitted equations can provide a reference to predict the average growth rate of CO_2 hydrates in the C1-C4 particle size systems under a driving force ranging from 2 to 3 MPa.

Analysis of the Influence Law of CO_2 Hydrate Heat of Decomposition

The complete decomposition of CO_2 hydrate requires the absorption of a large amount of heat, and the heat of decomposition is an important parameter for carrying out the hydrate method of solidifying and storing CO_2 in mines, as well as an important basic value for the stable existence of CO_2 hydrate in the outburst coal body. Therefore, it is crucial to determine the value of the heat of decomposition of CO_2 hydrate solidification products in the outburst coal body and the influence of the driving force on its variation. For this reason, in this paper, on the basis of the average calorific value of decomposition of CO_2 hydrate in the C1~C4 system using the Clausius-Clapeyron equation (Xie et al., 2020), the total heat of decomposition of

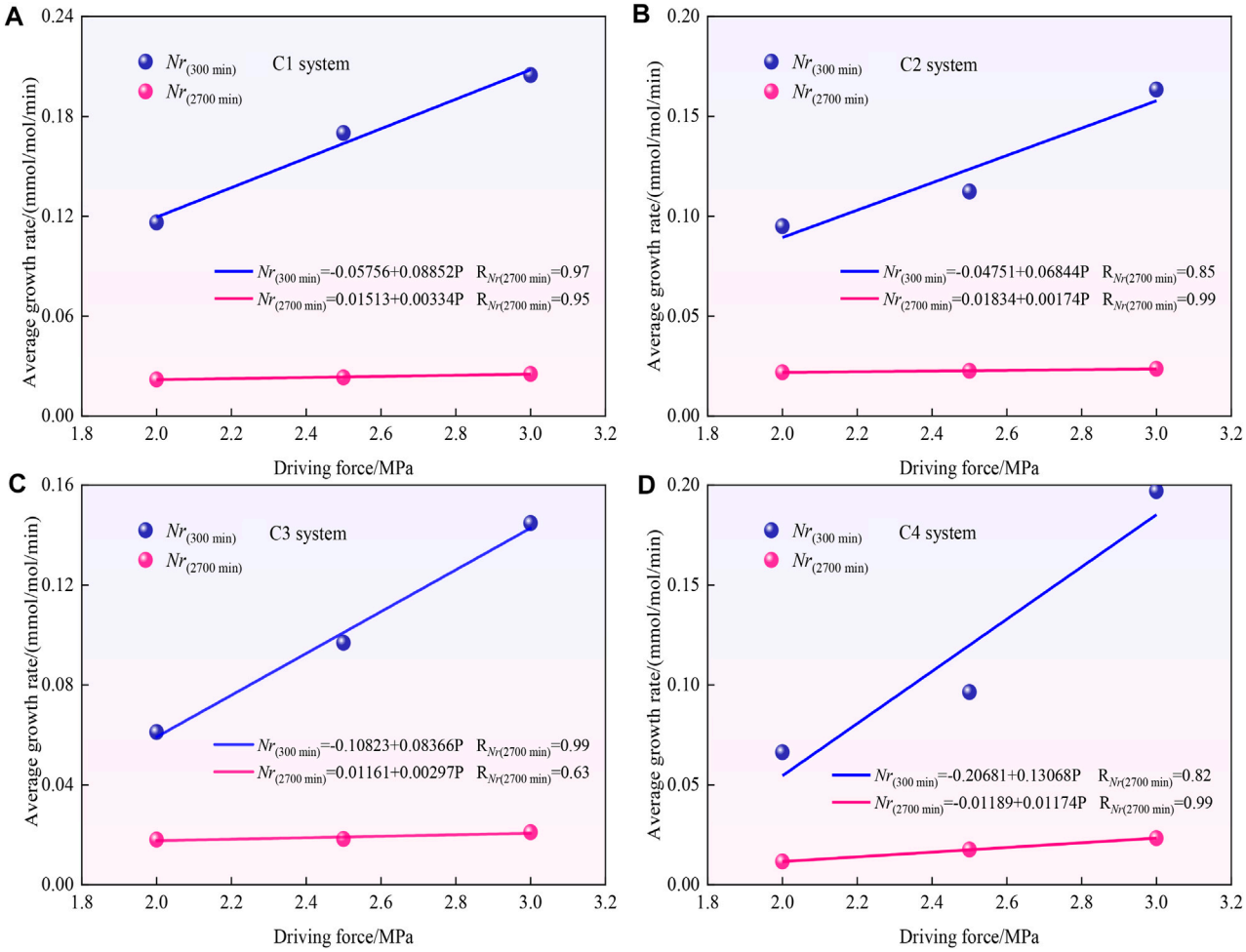

FIGURE 8 | Fitted plot of the average growth rate of CO_2 hydrates versus driving force in the C1-C4 systems.

TABLE 3 | Results of fitting the average growth rate of CO_2 hydrate versus driving force in the C1-C4 systems.

Medium	Fitting formula	Correlation coefficient	Fitting correlation
C1	$Nr_{(300\ min)}$ = −0.05756 + 0.08852P	$R_{Nr\ (300\ min)}$ = 0.97	extremely strong correlation
	$N_{r(2700\ min)}$ = 0.01513 + 0.00334P	$R_{Nr\ (2700\ min)}$ = 0.95	extremely strong correlation
C2	$N_{r(300\ min)}$ = -0.04751 + 0.06844P	$R_{Nr\ (300\ min)}$ = 0.85	strong correlation
	$N_{r(2700\ min)}$ = 0.01834 + 0.00174P	$R_{Nr\ (2700\ min)}$ = 0.99	extremely strong correlation
C3	$N_{r(300\ min)}$ = -0.10823 + 0.08366P	$R_{Nr\ (300\ min)}$ = 0.99	extremely strong correlation
	$N_{r(2700\ min)}$ = 0.01161 + 0.00297P	$R_{Nr\ (2700\ min)}$ = 0.63	general correlation
C4	$N_{r(300\ min)}$ = −0.20681 + 0.13068P	$R_{Nr\ (300\ min)}$ = 0.82	strong correlation
	$N_{r(2700\ min)}$ = −0.01189 + 0.01174P	$R_{Nr\ (2700\ min)}$ = 0.99	extremely strong correlation

Note: The medium comprises coal particles of C1: 0.425~0.850; C2: 0.250~0.425; C3: 0.180~0.250; C4: 0~0.180.

CO_2 hydrates in the different systems is obtained with **Eqn. 5**, and the experimental results are listed in **Table 4**.

$$\Delta H_{diss_{total}} = \Delta N_t \cdot \Delta H_{diss_{average}} \quad (5)$$

Where $\Delta H_{diss_{total}}$ is the total heat of decomposition of CO_2 hydrates (J) and $\Delta H_{diss_{average}}$ is the average heat of decomposition of the CO_2 hydrate system (kJ/mol).

Figure 9 shows a comparison of the heat of decomposition of CO_2 at the end of the hydration curing reaction under the different driving forces and four particle sizes of coal particles. The figure shows that the heat of decomposition of CO_2 hydrates gradually increases with increasing driving force in the same medium, and the heat required for complete decomposition increasingly stabilizes. This occurs because in the same coal

TABLE 4 | Total heat of decomposition of CO_2 hydrates in coal particles under the different driving forces.

Experimental system	Feed Gas	Medium	Particle size d/Mm	Average heat of decomposition/ kJ·mol^{-1}	Driving force ΔP/MPa	Gas consumption Nt/ (mmol/mol)	Total heat of decomposition/J
I-1-1	CO_2	C1	0.425~0.850	47.87	2	59.3	2838.69
I-1-2					2.5	62.6	2996.66
I-1-3					3	68.3	3269.52
I-2-1		C2	0.250~0.425	34.27	2	59	2021.93
I-2-2					2.5	61.1	2093.88
I-2-3					3	63.7	2183.00
I-3-1		C3	0.180~0.250	41.63	2	48.5	2019.06
I-3-2					2.5	49.2	2048.20
I-3-3					3	56.5	2352.10
I-4-1		C4	0~0.180	46.17	2	31.1	1435.89
I-4-2					2.5	0~0.18047.5	2193.08
I-4-3					3	62.8	2899.48

Note: The medium comprises coal particles of C1: 0.425~0.850; C2: 0.250~0.425; C3: 0.180~0.250; C4: 0~0.180.

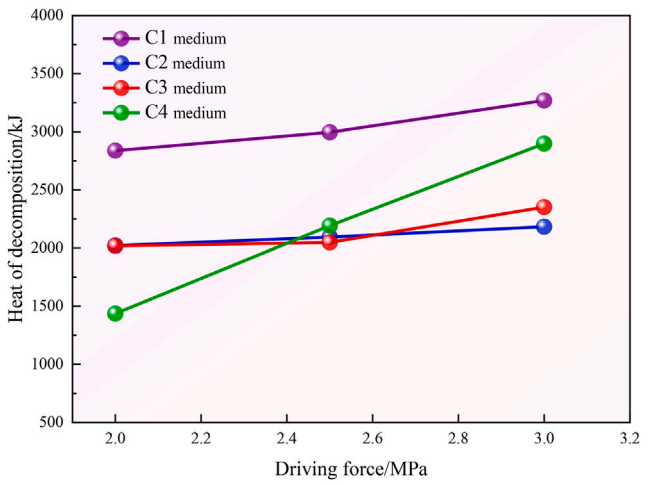

FIGURE 9 | Comparison of the heat of decomposition of CO_2 hydrates in the C1-C4 systems.

particle system, the total gas–liquid contact area is almost the same, and under the effect of a high driving force, more guest CO_2 molecules enter the deep coal particle reaction system through the surface layer to participate in the reaction. The other reason is that under the effect of a high driving force, the initial armor effect of the reaction system is mitigated, and more gas molecules participate in the reaction. Under the same driving force, the heat required for the decomposition of CO_2 hydrates in medium C1 is the highest and exhibits the highest heat of decomposition, indicating that the presence of CO_2 hydrates in medium C1 is relatively consistent.

CONCLUSION

By conducting comparative experimental studies on the growth kinetics of CO_2 hydrates in coal particles under three driving force conditions, the variations in CO_2 hydrate gas consumption, growth rate, total heat of decomposition and other effects were studied, and mechanisms and conclusions regarding the influence of the driving force on the growth kinetics of CO_2 hydrates in coal particles were obtained.

1) In the same particle size system, with increasing driving force, the nucleation time of hydrates in each system does not follow the same shortening pattern, and the effect of the different driving forces on the gas consumption of CO_2 hydrates is different. Under the three driving forces, the gas consumption of CO_2 hydrates was ranked as $\Delta N_{t,3\ MPa} > \Delta N_{t,2.5\ MPa} > \Delta N_{t,2\ MPa}$, and it could be concluded that the gas consumption of CO_2 hydrates increased with increasing driving force. By analyzing the effect of the different driving forces on CO_2 hydrate generation, it is concluded that there exists a critical value regarding the effect of the driving force on CO_2 hydrate generation in coal particles with the change in particle size, above which the effect of the driving force on CO_2 hydrate generation gradually decreases with decreasing particle size, and below which the effect of the driving force on CO_2 hydrate generation gradually intensifies with decreasing particle size.
2) Under the same temperature conditions, increasing the driving force of the CO_2 hydrate generation process in the same particle size system can increase the growth rate of CO_2 hydrates, and the driving force exerts a more obvious effect on the average growth rate at the early stage of synthesis. Under the same driving force conditions, the average growth rate of CO_2 hydrates decreases overall with decreasing coal particle size, but with increasing driving force, the variation in the average growth rate gradually decreases or the average growth rate even increases. Linear regression was employed to fit an equation of the relationship between the driving force and the average growth rate in each particle size system to provide a reference to predict the average growth rate of CO_2 hydrates in the C1-C4 particle size systems under a driving force ranging from 2~3 MPa.

3) During the growth of CO_2 hydrates in the coal particle system, the obstruction of CO_2 gas diffusion and migration within the coal particles due to the decrease in particle size is the main factor impacting the process of CO_2 hydrate generation. However, with decreasing particle size, the promoting effects, such as the increase in specific surface area and driving force of the coal particles, are strengthened and gradually become stronger than the hindering effects and dominate the factors promoting CO_2 hydrate generation in coal particles.
4) In the same medium, the heat of decomposition of CO_2 hydrates gradually increases with increasing driving force, and more heat is required for complete decomposition, which remains relatively stable. The heat required for the decomposition of CO_2 hydrates in the C1 medium is the highest and exhibits the highest total heat of decomposition, indicating that the presence of CO_2 hydrates in the C1 medium remains relatively constant.

DATA AVAILABILITY STATEMENT

The original contributions presented in the study are included in the article/Supplementary Material, further inquiries can be directed to the corresponding author.

AUTHOR CONTRIBUTIONS

LC: Thesis writing. CR: The data processing. ZB: Writing guidance. WQ: The experiment design. ZQ: The data analysis. WQ: The data analysis.

FUNDING

The work reported in this paper was funded by the National Natural Science Foundation of China under NSFC Contract No. U21A20111, 51704103, 51774123, 51974112, 51804105.

REFERENCES

Bai, Y., Cao, G., An, H., and Zhang, H. (2020). Generation Laws and Distribution Characteristics of Carbon Dioxide Hydrate in a Reaction Kettle. *Exp. Therm. Fluid Sci.* 116, 110125–125. doi:10.1016/j.expthermflusci.2020.110125

Black, D. J. (2019). Review of Coal and Gas Outburst in Australian Underground Coal Mines. *Int. J. Min. Sci. Technol.* 29 (06), 815–824. doi:10.1016/j.ijmst.2019.01.007

Cao, X. W., Yang, K. R., Xia, W. Z., Tang, G. X., and Bian, J. (2021). Dissociation Experiment and Dissociation Rate Model of CO_2 Hydrate[J]. *Nat. Gas. Ind.* 41 (07), 152–159. doi:10.3787/j.issn.1000-0976.2021.07.017

Dai, M. L., Sun, Z. G., Li, J., Li, C. M., and Huang, H. F. (2020). Research on Promotion Technology for Gas Storage in Hydrate[J]. *Chem. Industry Eng. Prog.* 39 (10), 3975–3986. doi:10.16085/j.issn.1000-6613.2020-0023

Fan, S. S., You, S. L., Lang, X. M., Wang, Y. H., Li, W. T., Liu, Y. Z., et al. (2020). Separation and Capture Carbon Dioxide by Clathrate-Hydrate Membranes: a Review[J]. *Chem. Industry Eng. Prog.* 39 (04), 1211–1218. doi:10.16085/j.issn.1000-6613.2019-1292

Hou, Z. J., and Lu, J. (2000). *On Key Stratum Team of Shallow seam[J]*. Xi'an: Journal of Xi'an University of Science and Technology, 5–8.

Hu, H. Z. (2022). *Energy Supply Is Effective, Energy Structure Continues to Be optimized[EB/OL*. [2022-04-20] Available at: http://www.stats.gov.cn/ztjc/zthd/lhfw/2022/lh_sjjd/202202/t20220228_1828037.html.

Kang, S.-P., and Lee, J.-W. (2010). Kinetic Behaviors of CO2 Hydrates in Porous Media and Effect of Kinetic Promoter on the Formation Kinetics. *Chem. Eng. Sci.* 65 (5), 1840–1845. doi:10.1016/j.ces.2009.11.027

Li, L. L., Zhao, J. Z., Li, H. T., Zhang, L. H., Fan, S. S., Li, Q. P., et al. (2019). A Newly Fitted Thermodynamic Model for Capture of CO_2 from Flue Gas by Hydrate Method[J]. *Nat. Gas. Ind.* 39 (4), 104–110. doi:10.3787/j.issn.1000-0976.2019.04.014

Li, W., Cheng, Y. P., Yang, Y. F., Wang, L. G., Chen, H. D., and Yang, Y. K. (2011). Research on the Genesis and Accumulation of Carbon Dioxide in the Yaojie Coalfield[J]. *J. China Univ. Min. Technol.* 40 (2), 190–195.

Liu, N., Zhang, Y. N., Liu, X. T., and You, L. T. (2015). Experimental Study on the Formation Characteristics of CO_2 Hydrate in Nanofluid[J]. *J. Refrig.* 36 (2), 41–45doi. doi:10.3969/j.issn.0253-4339.2015.02.041

Mech, D., Gupta, P., and Sangwai, J. S. (2016). Kinetics of Methane Hydrate Formation in an Aqueous Solution of Thermodynamic Promoters (THF and TBAB) with and without Kinetic Promoter (SDS). *J. Nat. Gas Sci. Eng.* 35, 1519–1534. doi:10.1016/j.jngse.2016.06.013

Montazeri, V., Rahimi, M., and Zarenezhad, B. (2019). Energy Saving in Carbon Dioxide Hydrate Formation Process Using Boehmite Nanoparticles. *Korean J. Chem. Eng.* 36 (11), 1859–1868. doi:10.1007/s11814-019-0375-y

Seo, Y.-T., Moudrakovski, I. L., Ripmeester, J. A., Lee, J.-w., and Lee, H. (2005). Efficient Recovery of CO2 from Flue Gas by Clathrate Hydrate Formation in Porous Silica Gels. *Environ. Sci. Technol.* 39 (7), 2315–2319. doi:10.1021/es049269z

Si, L., Wei, J., Xi, Y., Wang, H., Wen, Z., Li, B., et al. (2021). The Influence of Long-Time Water Intrusion on the Mineral and Pore Structure of Coal. *Fuel* 290, 119848. doi:10.1016/j.fuel.2020.119848

Si, L., Zhang, H., Wei, J., Li, B., and Han, H. (2021). Modeling and Experiment for Effective Diffusion Coefficient of Gas in Water-Saturated Coal. *Fuel* 284, 118887. doi:10.1016/j.fuel.2020.118887

Sun, J. Y., Liu, L. L., Wang, X. W., Wang, F. F., and Liu, C. L. (2015). Xperimental Study on the Replacement of Methane Hydrate in Sediments with CO_2. *J.* 35 (08), 56–62. doi:10.3787/j.issn.1000-0976.2015.08.008

Tao, M. X., Xu, Y. C., Ma, Y. Z., and Chen, F. Y. (1992). On Outbursts of Carbon Dioxide in Coal Mines[J]. *Adv. Earth Sci.* (05), 40–44.

Wang, L. J., Sun, D. S., Zhang, L. R., and Zhou, G. W. (2009). Application of *In-Situ* Stress Measurement on Bursts Disasters of Rock and CO_2 in Coal Mine[J]. *J. China Coal Soc.* 34 (01), 8–32.

Wu, D. M., Zhao, Y. M., Cheng, Y. P., and An, F. H. (2010).P Index with Different Gas Compositions for Instantaneous Outburst Prediction in Coal Mines[J]. *Min. Sci. Technol.* 20 (05), 723–726. doi:10.1016/S1674-5264(09)60270-2

Wu, Q., Li, C. L., and Jiang, C. L. (2005). Discussion on Control Factors of Forming Gas Hydrate[J]. *J. China Coal Soc.* (03), 283–287.

Xie, W. J., Li, X. S., Zou, Y. N., and Xu, C. G. (2020). Characteristics of Carbon Dioxide Hydrate Formation and Decomposition with the System of Cyclopentane[J]. *Chem. Industry Eng. Prog.* 39 (01), 129–136. doi:10.16085/j.issn.1000-6613.2019-0627

Xu, L., and Jiang, C. (2017). Initial Desorption Characterization of Methane and Carbon Dioxide in Coal and its Influence on Coal and Gas Outburst Risk. *Fuel* 203, 700–706. doi:10.1016/j.fuel.2017.05.001

Yang, H. M., Xu, D. L., and Chen, L. W. (2016). Quantitative Study on Displacement-Replacement of Methane in Coal through CO2 Injection [J]. *J. Saf. Sci. Technol.* 12 (05), 38–42. doi:10.11731/j.issn.1673-193x.2016.05.007

ZareNezhad, B., Mottahedin, M., and Varaminian, F. (2015). Experimental and Theoretical Investigations on the Enhancement of Methane Gas Hydrate Formation Rate by Using the Kinetic Additives. *Petroleum Sci. Technol.* 33 (8), 857–864. doi:10.1080/10916466.2015.1010042

Zhang, X. M., Li, J. P., Wu, Q. B., Wang, C. L., and Nan, J. H. (2015). Experimental Study on the Formation Characteristic of CO_2 Hydrate in Porous Media below the Freezing Point[J]. *J. China Petroleum Process. Petrochem. Technol.* 17 (3), 32–38.

Zheng, J., Bhatnagar, K., Khurana, M., Zhang, P., Zhang, B.-Y., and Linga, P. (2018). Semiclathrate Based CO2 Capture from Fuel Gas Mixture at Ambient Temperature: Effect of Concentrations of Tetra-N-Butylammonium Fluoride

(TBAF) and Kinetic Additives. *Appl. Energy* 217 (February), 377–389. doi:10.1016/j.apenergy.2018.02.133

Zheng, J., Loganathan, N. K., and Linga, P. (2019). Natural Gas Storage via Clathrate Hydrate Formation: Effect of Carbon Dioxide and Experimental Conditions. *Energy Procedia* 158, 5535–5540. doi:10.1016/j.egypro.2019.01.590

Zhong, D.-L., Ding, K., Lu, Y.-Y., Yan, J., and Zhao, W.-L. (2016). Methane Recovery from Coal Mine Gas Using Hydrate Formation in Water-In-Oil Emulsions. *Appl. Energy* 162, 1619–1626. doi:10.1016/j.apenergy.2014.11.010

Conflict of Interest: The authors declare that the research was conducted in the absence of any commercial or financial relationships that could be construed as a potential conflict of interest.

Publisher's Note: All claims expressed in this article are solely those of the authors and do not necessarily represent those of their affiliated organizations, or those of the publisher, the editors and the reviewers. Any product that may be evaluated in this article, or claim that may be made by its manufacturer, is not guaranteed or endorsed by the publisher.